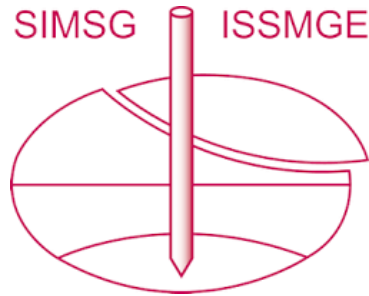


INTERNATIONAL SOCIETY FOR SOIL MECHANICS AND GEOTECHNICAL ENGINEERING



This paper was downloaded from the Online Library of the International Society for Soil Mechanics and Geotechnical Engineering (ISSMGE). The library is available here:

<https://www.issmge.org/publications/online-library>

This is an open-access database that archives thousands of papers published under the Auspices of the ISSMGE and maintained by the Innovation and Development Committee of ISSMGE.

FEM simulation of elasto-visco-plastic stress-strain behavior of stiff geo-materials

Simulation FEM des comportement de la tension élasto-visco-plastique des matériaux géologiques

M.S.A.Siddiquee, S.J.M.Yasin & E.Hoque – Department of Civil Engineering, Bangladesh University of Engineering and Technology, Dhaka, Bangladesh

F.Tatsuoka – University of Tokyo, Tokyo, Japan

ABSTRACT: A modeling of time-dependent (viscous) shear stress and shear strain behavior of clean sands in drained plane strain compression tests is presented. The general three-component model is used as the framework for constitutive modeling. A viscous model is developed to incorporate decaying properties of the viscous response of sand taking place by a change in the strain rate, called the TESRA (Temporary Effects of Strain Rate and Acceleration) model

1 INTRODUCTION

The paper describes a general elasto-viscoplastic model, called the TESRA model, formulated within the framework of classical three-component model and explains its implementation within the scope of generalized elasto-plastic isotropic strain-hardening Finite Element code. The TESRA model states the scaling of the shear stress of soil according to the instantaneous rate of irrecoverable strain and strain rate and decay of the viscous effects. The model can be easily integrated analytically or numerically in one-dimensional cases. But the integration scheme in FEM analysis needs some specific considerations. Choice of suitable invariant parameters is the key to the implementation of the model into a FEM code. The model has been successfully integrated with an existing FEM code. Some example problems have been solved with FEM. The FEM code can predict the time-dependent behavior of a wide variety of geomaterials quite accurately without spending any extra computational time or storage.

2 FUNDAMENTAL THEORY

2.1 Three-component viscous model

The following specific model (the new isotach model) within the framework of the general three-component model is known to be relevant to several types of geomaterials, including soft clays and soft rocks (Tatsuoka et al., 2000b):

$$\sigma^v = \sigma^f(\dot{\epsilon}^{ir}) + \sigma^v(\dot{\epsilon}^{ir}, \dot{\epsilon}^{ir}) \quad (1a)$$

$$\sigma^v(\dot{\epsilon}^{ir}, \dot{\epsilon}^{ir}) = \sigma^v(\dot{\epsilon}^{ir}) \cdot g_v(\dot{\epsilon}^{ir}) \quad (1b)$$

$$\sigma = \sigma^f(\dot{\epsilon}^{ir}) \cdot \{1 + g_v(\dot{\epsilon}^{ir})\} \quad (1c)$$

where $g_v(\dot{\epsilon}^{ir})$ is the viscosity function, which is always zero or positive and is given as follows for any strain (ϵ^{ir}) or stress (σ^f) path (with or without cyclic loading):

$$g_v(\dot{\epsilon}^{ir}) = \alpha \cdot \left[1 - \exp\left\{1 - \left(\frac{|\dot{\epsilon}^{ir}|}{\dot{\epsilon}_p^{ir}} + 1\right)^m\right\}\right] \quad (\geq 0) \quad (2)$$

2.2 Formulation of TESRA model

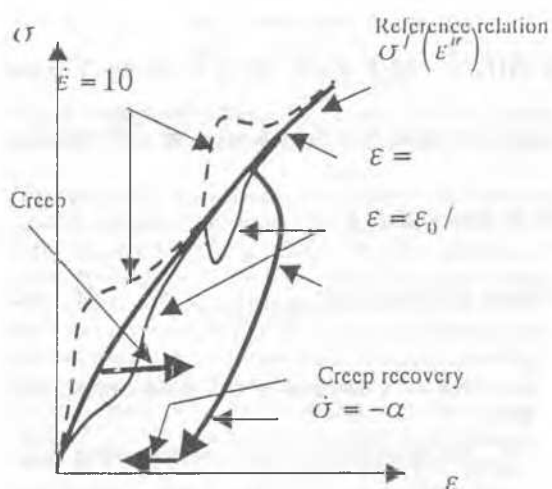


Figure 1. Behavior of the TESRA model.

Eq. 1b can be rewritten as follows:

$$\sigma^v = \int_{\tau=\epsilon_1^{ir}}^{\epsilon^{ir}} [d\sigma^v]_{(\tau)} = \int_{\tau=\epsilon_1^{ir}}^{\epsilon^{ir}} [d\{\sigma^f \cdot g_v(\dot{\epsilon}^{ir})\}]_{(\tau)} \quad (3a)$$

$$= \int_{\tau=\epsilon_1^{ir}}^{\epsilon^{ir}} \left[\left(\frac{\partial \sigma^f}{\partial \epsilon^{ir}} \right) \cdot g_v(\dot{\epsilon}^{ir}) + \sigma^f \cdot \left(\frac{\partial g_v(\dot{\epsilon}^{ir})}{\partial \dot{\epsilon}^{ir}} \right) \cdot \dot{\epsilon}^{ir} \right]_{(\tau)} \cdot d\tau \quad (3b)$$

$$(\sigma^v \geq 0)$$

where $\sigma^v (\geq 0)$ is the current viscous stress component, where $\epsilon^{ir} = \epsilon^{ir}$; $[d\sigma^v]_{(\tau)}$ is the viscous effect on the stress that took place when $\epsilon^{ir} = \tau$; ϵ_1^{ir} is the strain at the start of integration, where $\sigma^v = 0$; the first term of the right-hand side of Eq. 3b represents the component of the increment $d\sigma^v$ as

where;

1. $|d\varepsilon^{ir}|$ is the absolute value of irreversible strain increment $d\varepsilon^{ir}$;
2. σ_r is the value of σ^f at the latest stage where the sign of $d\varepsilon^{ir}$ was changed;
3. $[\sigma^v]_{(\varepsilon^{ir}-\Delta\varepsilon^{ir})}$ is the viscous stress at one step before where the irreversible strain is equal to $\varepsilon^{ir} - \Delta\varepsilon^{ir}$;
4. $\Delta\varepsilon^{ir}$ is the difference in the irreversible strain between the current step and the step immediately before $\Delta\varepsilon^{ir}$; and
5. $\Delta\{(\sigma^f - \sigma_r) \cdot g_v(\dot{\varepsilon}^{ir})\}$ is the difference in the value of $(\sigma^f - \sigma_r) \cdot g_v(\dot{\varepsilon}^{ir})$ between the current step and the step immediately before, given as

$$\Delta\{(\sigma^f - \sigma_r) \cdot g_v(\dot{\varepsilon}^{ir})\} = \Delta\{(\sigma^f - \sigma_r) \cdot g_v(\dot{\varepsilon}^{ir})\} + (\sigma^f - \sigma_r) \cdot \Delta g_v(\dot{\varepsilon}^{ir}) \quad (9)$$

The term $\Delta\{(\sigma^f - \sigma_r) \cdot g_v(\dot{\varepsilon}^{ir})\} \cdot r_1^2$ in Eq. 7 is the viscous effects that took place for this range of $\Delta\varepsilon^{ir}$ that has decayed by an amount of r_1^2 .

So, for known values of $[\sigma^v]_{(\varepsilon^{ir}-\Delta\varepsilon^{ir})}$, $\Delta\varepsilon^{ir}$, Δt (i.e., $\dot{\varepsilon}^{ir} = \frac{\Delta\varepsilon^{ir}}{\Delta t}$) and ε^{ir} , the value of σ^v at the current state,

where $\varepsilon^{ir} = \varepsilon^{ir}$, can be obtained by Eq. 7, without doing an integration.

Repeating this procedure from the start of loading, the whole stress-strain-time relationship can be obtained for any given history of strain or stress with or without cyclic loading.

4.2 Implementation into FEM Code

An existing nonlinear FEM code will be used, which is based on the matrix-free dynamic relaxation technique (Siddiquee et al., 1999), highly optimized for very fast and accurate computation of highly nonlinear equations emerging from material nonlinearity. Due to the specialty of the DR (Dynamic Relaxation), the following steps to be considered carefully for relevant implementation of the TESRA model into the FEM code.

Computation of irrecoverable strain rate

In case of modeling granular materials, obviously for the rate of effective plasticity parameter, k , the primary candidate is the rate of the second irrecoverable strain invariant. This is a scalar quantity and it is already being calculated in the FEM code. But there is one problem with this; i.e., as it is always positive, it cannot be used in unloading situations. So the following variable is used in the present formulation:

$$k = \varepsilon_1^{ir} - \varepsilon_3^{ir} \quad \dot{k} = \frac{k}{dt} \quad (10)$$

Selection of current stress variable

Stress ratio, $R = \sigma_1 / \sigma_3$ is selected to represent the current shear stress level.

4.3 Pseudo-algorithm

The following steps are followed to calculate the viscous stress:

1. Calculation of trial strain
2. Stress increment calculation by the hypo-elastic constitutive law (Hoque, 1998):

$$E_h = E_0 \sigma_h^n, \quad E_v = E_0 \sigma_v^n$$

Elasto-plastic solution (without viscous effects) is calculated. Plastic consistency conditions and a flow rule are applied and each trial stress is integrated back to the inviscid yield surface, f^I .

$$df^I(\sigma_{ij}, k) = 0, \quad d\varepsilon_{ij}^p = \lambda \frac{\partial \phi}{\partial \sigma_{ij}}$$

(a) The current strain rate is calculated from the plastic strain rate generated in the previous step.

(b) The iterating inviscid stress is further corrected by the TESRA Model Eq. (7).

3. Nodal forces are calculated and compared with the applied load and the iteration continues, starting from 1 again, until the equilibrium is reached.

5 NUMERICAL SIMULATION

5.1 Problem definition

In order to perform numerical simulations, the following one-element configuration has been devised. The material is Toyoura sand with a void ratio, $e=0.66$ and a confining pressure, $\sigma_3=98$ kPa.

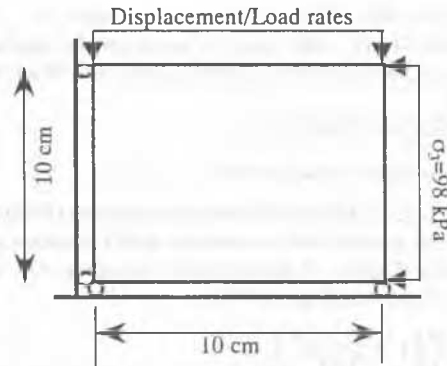


Figure 3. Definition of the problem.

5.2 Material model

An isotropically strain-hardening-softening elasto-visco-plastic model is used here (Siddiquee 1999). Essentially this is a non-associated flow analysis and the relevant dilatancy is modeled by adapting the Rowe's stress-dilatancy relationship. The growth function represented by strain hardening is modeled by the General Hyperbolic Equation (GHE) (Siddiquee 1999). The viscous model parameters those were employed: $\alpha = 0.23$, $m=0.045$, $\varepsilon_0^{ir} = 0.0001$ and $r_1=0.3$ (the TESRA model).

the effect of the irreversible strain increment $d\varepsilon^{ir}$ when loading continues at a constant $\dot{\varepsilon}^{ir}$ (i.e., the effect of irreversible strain rate); and the second term represents the component of the

increment $d\sigma^v$ as the effect of the increment of irreversible strain rate $d\dot{\epsilon}^{ir}$ applied at a certain constant $\dot{\epsilon}^{ir}$ (i.e., the effect of irreversible strain acceleration).

2.2.1 Introducing the decay function

Granular material always shows a tendency with straining of decay of the stress jump that takes place by a strain-jump (Fig. 1). To model this phenomenon, the decay function $g_{decay}(\epsilon - \tau) = r_1$ is incorporated in to Eq. (3) to obtain:

$$\sigma^v = \int_{\tau=\dot{\epsilon}^{ir}}^{\dot{\epsilon}^{ir}} \left[\left(\frac{\partial \sigma^f}{\partial \dot{\epsilon}^{ir}} \right) \cdot g_v(\dot{\epsilon}^{ir}) + \sigma^f \cdot \left(\frac{\partial g_v(\dot{\epsilon}^{ir})}{\partial \dot{\epsilon}^{ir}} \right) \cdot \frac{\dot{\epsilon}^{ir}}{\dot{\epsilon}^{ir}} \right] \cdot r_1(\dot{\epsilon}^{ir} - \tau) \cdot d\tau \quad (4)$$

where r_1 is a positive constant less than 1.0. In case $r_1 = 1.0$, Eq. 4 becomes Eq. 3, therefore Eq. 1.

2.3 Formulation of the General TESRA model

Some materials show an increasing degree of decay with the increase in the stress level. For these cases, the decay function is made dependent on the irreversible strain as:

$$\sigma^v = \int_{\tau=\dot{\epsilon}^{ir}}^{\dot{\epsilon}^{ir}} \left[\left(\frac{\partial \sigma^f}{\partial \dot{\epsilon}^{ir}} \right) \cdot g_v(\dot{\epsilon}^{ir}) + \sigma^f \cdot \left(\frac{\partial g_v(\dot{\epsilon}^{ir})}{\partial \dot{\epsilon}^{ir}} \right) \cdot \frac{\dot{\epsilon}^{ir}}{\dot{\epsilon}^{ir}} \right] \cdot r(\dot{\epsilon}^{ir})^{r-1} \cdot d\tau \quad (5)$$

where $r(\dot{\epsilon}^{ir})$ means that the decay parameter r decreases with $\dot{\epsilon}^{ir}$.

The following function was chosen for $r(\dot{\epsilon}^{ir})$ to simulate the primary loading stress-strain behaviour:

$$r(\dot{\epsilon}^{ir}) = r_i \quad \text{at } \dot{\epsilon}^{ir} = 0 \quad (6a)$$

$$r(\dot{\epsilon}^{ir}) = \frac{r_i + r_f}{2} + \frac{r_i - r_f}{2} \cdot \cos \left\{ \pi \cdot \left(\frac{\dot{\epsilon}^{ir}}{c} \right)^n \right\} \quad \text{for} \quad 0 \leq \dot{\epsilon}^{ir} \leq c \quad (6b)$$

$$r(\dot{\epsilon}^{ir}) = r_f \quad \text{for } \dot{\epsilon}^{ir} \geq c \quad (6c)$$

Figure 4. Stress-strain behavior of the general TESRA model with variable decay function.

where r_i and r_f are the initial and ultimate values of r , where $0 \leq r_f \leq r_i \leq 1.0$; and c and n are positive constants.

For primary loading cases, all of the new isotach model, the TESRA model and the general TESRA model can be represented by a set of common equations (Eqs. 4, 5 and 6) using the following different values of r_i and c :

$c = \infty$ and $r_i = 1.0$ (always $r = 1.0$): no decay (the new isotach model);

$c = \infty$ and $0 < r_i < 1.0$ (always $r = r_i < 1.0$) (the TESRA mode); and

$0 < c < \infty$ and $0 < r_f < r_i < 1.0$ (the general TESRA model).

3 VALIDATION OF THE MODEL

Fig. 2 shows the relationship between the stress ratio $R = \sigma_v^i / \sigma_h^i$ and the shear strain $\gamma = \epsilon_v - \epsilon_h$ from a PSC test on Toyoura sand and its simulation by the TESRA model.

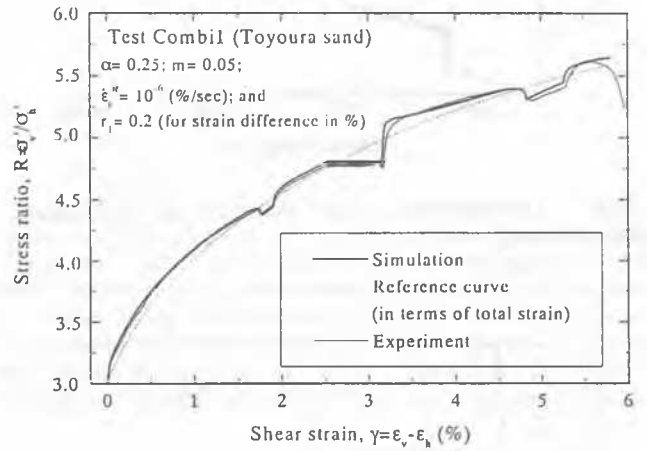


Fig. 2 Measured stress-strain relations for a drained PSC test ($e_0 = 0.730$) on Toyoura and its simulation by the TESRA model.

Toyouura sand, from Japan, is a quartz-rich sub-angular poorly-graded medium-sized sand with $D_{50} = 0.18$ mm, $U_c = 1.64$, $G_s = 2.65$, $e_{max} = 0.99$ and $e_{min} = 0.62$. The PSC specimen was rectangular-prismatic of 20 cm high, 16 cm long and 8 cm wide (in the σ_3 direction) with lubricated top and bottom ends. The specimen was prepared by pluviating air-dried sand particles through air and were then made saturated. The specimen was anisotropically consolidated at a stress ratio $R = 3.0$ and at a constant rate of axial strain, $\dot{\epsilon}_v = 0.0125$ %/min., from the initial stress state with $\sigma_h^i = 29$ kPa towards the final consolidation stress state with $\sigma_h^i = 392$ kPa. The axial strain rates during PSC loading was basically either 0.0005%/sec or 0.006%/sec. At several intermediate stages, the axial strain rate was increased and decreased at a constant rate, while one creep test was performed for about 24 hours. It can be seen that the test result is simulated very well by the TESRA model. The model parameters are shown in Fig. 2. The validation of the TESRA model is fully reported by Di Benedetto et al. (2000) and Tatsuoka et al. (2000b).

4 IMPLEMENTATION DETAILS

4.1 Numerical integration scheme

The basic TESRA equation (Eq. 4) can be generalized to include unloading-reloading cases as:

$$\sigma^v = \int_{\tau=\dot{\epsilon}^{ir}}^{\dot{\epsilon}^{ir}} [d\sigma^v]_{(\tau, \dot{\epsilon}^{ir}, h)} + \Delta\sigma^v \quad (7)$$

$$= [\sigma^v]_{(\tau, \dot{\epsilon}^{ir}, h)} \cdot r_1^{|\dot{\epsilon}^{ir}|} + \Delta\{(\sigma^v - \sigma_c) \cdot g_v(\dot{\epsilon}^{ir})\} \cdot r_1 \cdot \dot{\epsilon}^{ir}$$

$$g_{decay}(D) = r_1^D; \quad D = \int_{\tau}^{\dot{\epsilon}^{ir}} |d\dot{\epsilon}^{ir}| \quad (8)$$

5.3 FEM Analysis

The following two cases were simulated :

- 1) a displacement control test with varying displacement rates (Fig. 4); and

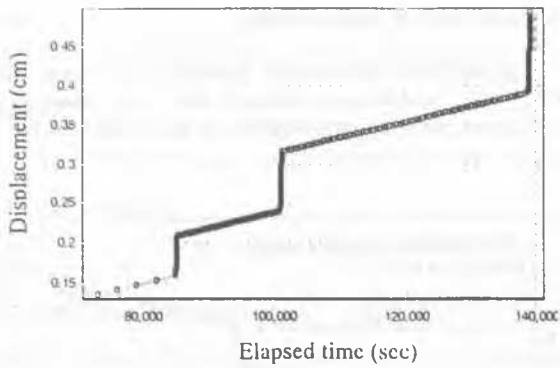


Figure 4. Displacement vs. time relationship for displacement control loading

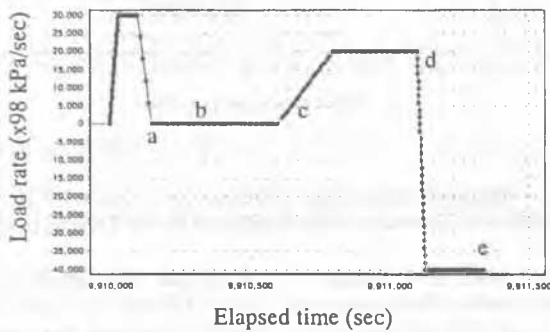


Figure 5. Load rate vs. time relationship Load control loading

2) a load control test with varying load rates (Fig. 5).

It may be seen from the results from the analysis (Figs. 6 and 7), while referring to Fig. 6, that the simulation is very realistic, in particular with the following phenomena;

- 1) temporary over- and under-shooting in the stress by a sudden increase and decrease in the displacement rate (i.e., strain rate) or the loading rate (i.e., stress rate); i.e., a sudden change in the stiffness immediately after a sudden change in the strain or stress rate, followed by a sudden change in the tangent stiffness and rejoining to the original stress-strain behaviour with subsequent loading;

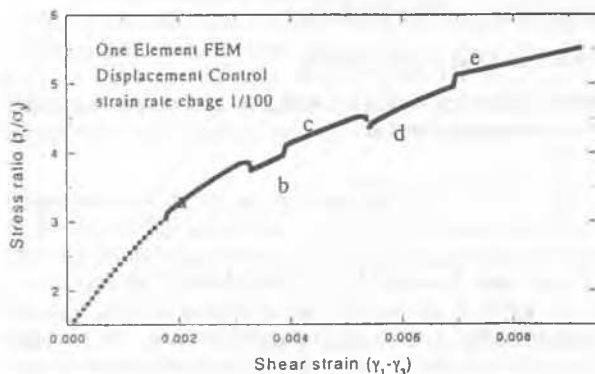


Figure 6. Stress-strain result obtained from FEM computation (Displacement-control).

- 2) creep behaviour, followed by very stiff behaviour when loading is resumed at a constant stress rate (Fig. 7); and continuation of the development of shear strain for a some stress

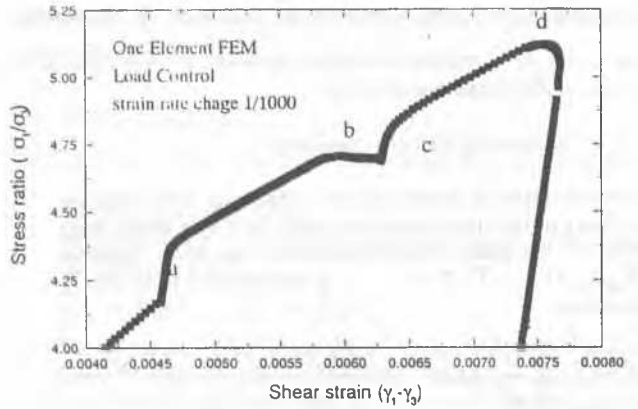


Figure 7. Stress-strain result obtained from FEM computation (Load-control).

range after the shear stress has started decreasing (from point d in Fig. 7), followed by a switching from an increase to a decrease in the shear strain in the course of stress decreasing.

6 CONCLUSIONS

The following conclusions can be drawn:

1. Time-dependent stress-strain behavior of granular materials is a function of previous and instantaneous strain-rate and acceleration.
2. With granular materials, the viscous effects on the stress value decay with the increase in the irreversible strain.
3. The above viscous features can be modeled and have been implemented in ordinary FEM codes without major modifications.

7 REFERENCES

- Di Benedetto, H. and Tatsuoka, F. 1997. Small strain behaviour of geomaterials: modelling of strain effects, *Soils and Foundations*, Vol.37, No.2, pp.127-138
- Di Benedetto, H., Tatsuoka, F. and Ishihara, M. 2000b.: Time-dependent deformation characteristics of sand and their constitutive modelling, *Soils and Foundations* (submitted).
- Hoque, E. and Tatsuoka, F. 1998. Anisotropy in the elastic deformation of materials", *Soils and Foundations*, *Soils and Foundations*, Vol.38, No.1, pp.163-179.
- Siddiquee, M.S.A., Tanaka, T., Tatsuoka, F., Tani, K. and Morimoto, T. 1999. FEM simulation of scale effect in bearing capacity of strip footing on sand", *Soils and Foundations*, Vol.39, No.4, pp.91-109.
- Tatsuoka, F., Uchimura, T., Hayano, K., Di Benedetto, H., Koseki, J. and Siddiquee, M.S.A. 2000a. Time-dependent deformation characteristics of stiff geomaterials in engineering practice", the Theme Lecture, *Proc. of the Second International Conference on Pre-failure Deformation Characteristics of Geomaterials, Torino, 1999* (Jamiolkowski et al., eds.), Balkema, Vol. 2 (to appear).
- Tatsuoka, F., Ishihara, M., Di Benedetto, H. and Kuwano, R. 2000b. Time-dependent deformation characteristics of geomaterials and their simulation, *Soils and Foundations* (submitted).
- Yasin, S.J.M. and Tatsuoka, F. 2000. Stress history-dependent deformation characteristics of dense sand in plane strain", *Soils and Foundations*, Vol.40, No.2, pp.55-74.